Wormhole Dynamics

2015 J. Phys.: Conf. Ser. 574 012056

(http://iopscience.iop.org/1742-6596/574/1/012056)

Journal of Physics: Conference Series **574** (2015) 012056 doi:10.1088/1742-6596/574/1/012056

Wormhole Dynamics

Hisa-aki Shinkai[1,2], **Takashi Torii** [3]

[1] Faculty of Information Science and Technology, Osaka Institute of Technology, Hirakata, Osaka 573-0196, Japan
[2] Computational Astrophysics Laboratory, Institute of Physical & Chemical Research (RIKEN), Hirosawa, Wako, Saitama, 351-0198 Japan
[3] Faculty of Engineering, Osaka Institute of Technology, Osaka, Osaka 535-8585, Japan

E-mail: hisaaki.shinkai@oit.ac.jp

E-mail: takashi.torii@oit.ac.jp

Abstract. Wormholes are theoretical products in general relativity, and are popular tools in science fictions. We know numerically the four-dimensional Ellis wormhole solution (the so-called Morris-Thorne's traversable wormhole) is unstable against an input of scalar-pulse from one side. We investigate this feature for higher-dimensional versions, both in n-dimensional general relativity and in Gauss-Bonnet gravity. We derived Ellis-type wormhole solution in n-dimensional general relativity, and found existence of unstable modes in its linear perturbation analysis. We also evolved it numerically in dual-null coordinate system, and confirmed its instability. The wormhole throat will change into black-hole horizon for the input of (relatively) positive energy, while it will change into inflationary expansion for (relatively) negative energy input. If we add Gauss-Bonnet terms (higher curvature correction terms in gravity), then wormhole tends to expand (or change to black-hole) if the coupling constant α is positive (negative).

1. Introduction

Wormhole is hypothetical object such as a short-cut tunnel connecting two points in space-time. The idea is essential in science fictions as a way for rapid interstellar travel, warp drives, and time machines. However, wormhole is also a theoretical research topic with long history.

The first appearance of a "tunnel structure" was in 1916 by Flamm [1] just after the discovery of Schwarzschild's black-hole solution. Einstein and Rosen [2] proposed a "bridge structure" between black-holes in order to obtain a regular solution without a singularity. The name "wormhole" was coined by John A. Wheeler in 1957, and its fantastic applications are popularized after the influential study of traversable wormholes by Morris and Thorne [3].

They considered "traversable conditions" for human travel through wormholes responding to Carl Sagan's idea for his novel *Contact*, and concluded that such a wormhole solution is available if we allow "exotic matter" (negative-energy matter).

The introduction of exotic matter sounds to be unusual for the first time, but such matter appears in quantum field theory and in alternative gravitational theories such as scalar-tensor theories. The Morris-Thorne solution is constructed with a massless Klein-Gordon field whose gravitational coupling takes the opposite sign to normal, which is found in Ellis's earlier work [4], so that we call it Ellis wormhole, hereafter. (See a review e.g. by Visser [5] for earlier works; See also e.g. Lobo [6] for recent works).

Ellis wormhole solution was studied in many contexts. Among them, we focus on its dynamical features. The first numerical simulation on its stability behavior was reported by one of the authors [7]. They use a dual-null formulation for spherically symmetric space-time integration, and observed that the wormhole is unstable against Gaussian pulses in either exotic or normal massless Klein-Gordon fields. The wormhole throat suffers a bifurcation of horizons and either explodes to form an inflationary universe or collapses to a black hole, if the total input energy is negative or positive, respectively. These basic behaviors were repeatedly confirmed by other groups [8, 9].

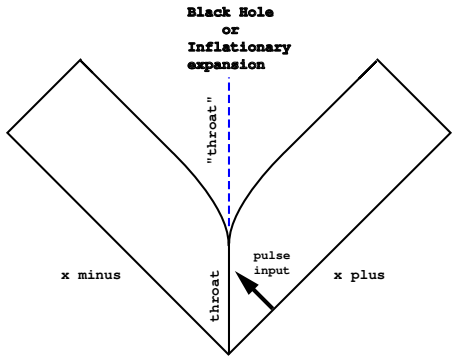

Figure 1. Partial Penrose diagram of the evolved space-time. Suppose we live in the right-side region and input a pulse to an Ellis-wormhole in the middle of the diagram. The wormhole throat suffers a bifurcation of horizons and either explodes to form an inflationary universe or collapses to a black hole, if the total input energy is negative or positive, respectively [7].

The changes of wormhole either to a black hole or an expanding throat supports an unified understanding of black holes and traversable wormholes proposed by Hayward [10]. His proposal is that the two are dynamically interconvertible, and that traversable wormholes are understandable as black holes under the existence of negative energy density.

In this article, we introduce our extensional works of [7], mainly its stability behavior in higher-dimensional space-time. The higher-dimensional theories such as string/M theories are applied for various unsolved problems in gravitational phenomena and cosmology, and gain new insights into them. We believe that wormholes will also give us new fundamental physical landscapes. We therefore demonstrate wormhole dynamics also in Gauss-Bonnet gravity, which is one of the modified gravity theory including higher-order corrections of curvatures, one of the string-motivated gravity theories.

Wormhole study in higher-dimensional space-time is not a new topic. We can find the articles from 80s [12, 13], and the recent studies are including higher-curvature terms (see e.g. [14] and [15] and references therein). Most of the researches concern the solutions and their energy conditions mainly, but to our knowledge there is no general discussion on the stability analysis of the solutions.

The main four contents in this article are: (a) constructing Ellis solutions in higher-dimensional general relativity, (b) stability analysis using linear perturbation method [16], (c) stability analysis using numerical evolution method, and (d) dynamical effects of Gauss-Bonnet coupling in 5-dimensional wormhole solution.

In §2, we derive the simplest wormhole solution with ghost scalar field in spherically symmetric, higher-dimensional space-time. We then study its stability using linear perturbation analysis, and find that there is at least one unstable mode in any dimensional space-time.

In §3, we try to confirm the prediction of instability using numerical evolutions. We implemented numerical code in [7] as it can treat higher-dimensional versions. We also demonstrate the wormhole structure in Gauss-Bonnet gravity theory.

2. Wormhole solutions in higher-dimensional general relativity

2.1. Field equations

We start from the n-dimensional Einstein-Klein-Gordon system

$$S = \int d^n x\sqrt{-g}\Big[\frac{1}{2\kappa_n^2}R - \frac{1}{2}\epsilon(\nabla\phi)^2 - V(\phi)\Big], \tag{1}$$

where κ_n^2 is a n-dimensional gravitational constant. The scalar field ϕ is the *normal* (or *ghost*) field if $\epsilon = 1$ (-1).

The metric of the space-time is assumed to be

$$ds^2 = -f(t,r)e^{-2\delta(t,r)}dt^2 + f(t,r)^{-1}dr^2 + R(t,r)^2 h_{ij}dx^i dx^j, \tag{2}$$

where $h_{ij}dx^i dx^j$ represents the line element of a unit $(n-2)$-dimensional constant curvature space with curvature $k = \pm 1, 0$ and volume Σ_k. In order to construct a static wormhole solution, we restrict the metric function as $f = f(r)$, $R = R(r)$, $\phi = \phi(r)$, and $\delta = 0$ in this subsection.

The Klein-Gordon equation becomes

$$\frac{1}{R^{n-2}}(R^{n-2}f\phi')' = -\epsilon\frac{dV}{d\phi}. \tag{3}$$

Hereafter, we construct the solution with the massless ghost scalar field ($V(\phi) = 0$ and $\epsilon = -1$). The Klein-Gordon equation (3) is integrated as

$$\phi' = \frac{C}{fR^{n-2}}, \tag{4}$$

where C is an integration constant. The Einstein equations are reduced to

$$\frac{(n-2)R'}{R}\Big[\frac{f'}{f} + \frac{(n-3)R'}{R}\Big] - \frac{(n-2)(n-3)k}{fR^2} = -\frac{\kappa_n^2 C^2}{f^2 R^{2(n-2)}}, \tag{5}$$

$$\frac{(n-2)R''}{R} = \frac{\kappa_n^2 C^2}{f^2 R^{2(n-2)}}. \tag{6}$$

The throat of the wormhole is at $r = 0$, and a is the radius of the throat, i.e. $R(0) = a$. The regularity conditions at the throat is written as $R(0) = a > 0$, and $f(0) = f_0 > 0$, where f_0 is a constant. Here we can assume $a = 1$ and $f_0 = 1$ without loss of generality, but we keep a in the equations in this section for later convenience. We assume the reflection symmetry with respect to the throat: $R'(0) = 0$, and $f'(0) = 0$. We also impose $\phi(0) = 0$ by a shift symmetry of the scalar field. With these conditions, the integration constant C is determined as

$$\kappa_n^2 C^2 = (n-2)(n-3)ka^{2(n-3)}. \tag{7}$$

This relation implies that there is no wormhole solution for the cases $k = 0$ and $k = -1$. Hence we investigate the spherically symmetric case $k = 1$.

The solution of Eqs. (4)–(6) is obtained as

$$f \equiv 1, \tag{8}$$

$$R' = \sqrt{1 - \Big(\frac{a}{R}\Big)^{2(n-3)}}, \tag{9}$$

$$\phi = \frac{\sqrt{(n-2)(n-3)}}{\kappa_n}a^{n-3}\int\frac{1}{R(r)^{n-2}}dr. \tag{10}$$

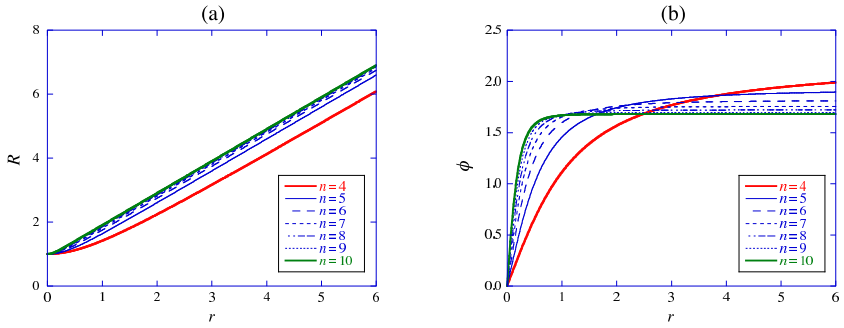

Figure 2. The n-dimensional wormhole solutions; (a) The circumference radius R and (b) the scalar field ϕ are plotted as a function of the radial coordinate r.

The eq. (9) is integrated to give

$$r(R) = -mB_z\Big(-m,\ \frac{1}{2}\Big) - \frac{\sqrt{\pi}\Gamma[1-m]}{\Gamma[m(n-4)]}, \tag{11}$$

where $m = 1/2(n-3)$ and $z = R^m$. $B_z(p,q)$ is the incomplete beta function defined by $B_z(p,q) := \int_0^z t^{p-1}(1-t)^{q-1}dt$. For $n = 4$, this solution reduces to Ellis's wormhole solution $f \equiv 1,\ R = \sqrt{r^2+a^2},\ \phi = \sqrt{2}\tan^{-1}(r/a)$.

At the throat

$$R''(a) = \frac{n-3}{a}, \quad \text{and} \quad \phi'(a) = \frac{\sqrt{(n-2)(n-3)}}{\kappa_n a}. \tag{12}$$

These indicate that the throat of the wormhole has larger curvature and the scalar field ϕ becomes steeper as n goes higher. We plotted these behaviors in Figure 2. For $n \to \infty$, the functions have the limiting solution, $R = r + a$ and $\phi = \pi/2$ $(r > 0)$.

2.2. Stability analysis

In this subsection, we investigate the linear stability of the higher-dimensional wormhole. We follow the analysis in [9], where the throat radius is not fixed since it is shown that the instability occurs by resolution of the degeneracy of a double trapping horizon [7].

We focus on the "spherical" modes, where the $(n-2)$-dimensional constant curvature space is not perturbed. In the time-dependent metric ansatz eq. (2) we write the perturbed functions as

$$f(t,r) = f_0(r) + \varepsilon f_1(r)e^{i\omega t}, \tag{13}$$
$$\delta(t,r) = \delta_0(r) + \varepsilon \delta_1(r)e^{i\omega t}, \tag{14}$$
$$R(t,r) = R_0(r) + \varepsilon R_1(r)e^{i\omega t}, \tag{15}$$
$$\phi(t,r) = \phi_0(r) + \varepsilon \phi_1(r)e^{i\omega t}, \tag{16}$$

where ε is an infinitesimal parameter, and the variables with subscript 0 denote the static solution.

By introducing the new variable,

$$\psi_1 = R_0^{\frac{n-2}{2}}\Big(\phi_1 - \frac{\phi_0'}{R_0'}R_1\Big), \tag{17}$$

the first-order equations give the single master equation,

$$-\psi_1'' + V(r)\psi_1 = \omega^2\psi_1, \tag{18}$$

with the potential,

$$V(r) = \frac{n-2}{2}\Big[\frac{n-3}{R_0^{2(n-2)}} + \frac{(n-4)R_0'^2}{2R_0^2}\Big] + \frac{2(n-3)^2}{R_0^{2(n-2)}R_0'^2}. \tag{19}$$

Here we have assumed $a = 1$. The variable ψ_1 is gauge invariant under the spherically symmetric ansatz. Since R_0' is zero at the throat and the potential V diverges there, we regularize the master equation (18).

Using the 0-mode solution of the master equtaion (18), $\bar{\psi}_1 = \left(R_0^{\frac{n-4}{2}}R_0'\right)^{-1}$, we define a pair of differential operators, $\mathcal{D}_\pm = \pm\frac{d}{dr} - \frac{\bar{\psi}_1'}{\bar{\psi}_1}$. Then the master equation, (18), can be written as

$$\mathcal{D}_-\mathcal{D}_+\psi_1 = \omega^2\phi_1. \tag{20}$$

Operating $\mathcal{D}_+$ from the left and defining the new variable $\Psi_1 = \mathcal{D}_+\psi_1$, we find the regularized master equation

$$-\Psi_1'' + W(r)\Psi_1 = \omega^2\Psi_1, \tag{21}$$

where

$$W(r) = -\frac{1}{4R_0^2}\Big[\frac{3(n-2)^2}{R_0^{2(n-3)}} - (n-4)(n-6)\Big]. \tag{22}$$

Now the potential function is regular everywhere. For $n = 4$, $W(r)$ has the minimum at the throat and is negative definite. For $n \geq 5$, $W(r)$ has the minimum at the throat, while it increases apart from the throat and becomes positive for large r.

We search eigenfunctions $\Psi_1(r)$ of eq. (21), and find that in any dimension n. There exists one negative eigenvalue for ω^2, which are listed in Table 1. The existence of the eigenfunction with negative ω^2 implies that the solution is unstable. We find large negative ω^2 for higher n, which indicates the timescale of instability becomes shorter.

Table 1. The negative eigenvalues ω^2.

n	ω^2	n	ω^2
4	− 1.39705243371511	10	−12.0442650147438
5	− 2.98495893027790	11	−13.9552091676647
6	− 4.68662054299460	20	−31.5751101285105
7	− 6.46258414126318	50	−91.3457759137153
8	− 8.28975936306259	100	− 191.283017729717
9	− 10.1535530451867		

3. Numerical evolutions of wormhole solutions

The purpose of this section is to confirm the prediction of instability of wormholes using numerical evolutions. We developed our numerical code as it can treat higher-dimensional versions. We also implemented it for studying the wormhole structure in Gauss-Bonnet gravity theory, which is one of the modified gravity theory including higher-order corrections of curvatures.

We begin describing Gauss-Bonnet theory briefly in §3.1, then explain our strategy in §3.2. The results will be shown in §3.3 and §3.4.

3.1. Einstein-Gauss-Bonnet gravity

Einstein-Gauss-Bonnet (EGB) gravity is derived from the superstring theory, with additional higher-order curvature correction terms to general relativity. Such higher-order corrections can be treated as an expansion of $\mathcal{R}$ in the action, but the Gauss-Bonnet term,

$$\mathcal{L}_{\rm GB} = \mathcal{R}^2 - 4\mathcal{R}_{\mu\nu}\mathcal{R}^{\mu\nu} + \mathcal{R}_{\mu\nu\rho\sigma}\mathcal{R}^{\mu\nu\rho\sigma}, \tag{23}$$

has good properties such that it is ghost-free combinations[11] and does not give higher derivative equations but an ordinary set of equations with up to the second derivative in spite of the higher curvature combinations.

The EGB action in n-dimensional space-time $(\mathcal{M}, g_{\mu\nu})$ is described as

$$S = \int_{\mathcal{M}} d^n X \sqrt{-g}\Big[\frac{1}{2\kappa^2}\left\{\alpha_{\rm GR}\left(\mathcal{R} - 2\Lambda\right) + \alpha_{\rm GB}\mathcal{L}_{\rm GB}\right\} + \mathcal{L}_{\rm matter}\Big], \tag{24}$$

where κ^2 is the n-dimensional gravitational constant, $\mathcal{R}$, $\mathcal{R}_{\mu\nu}$, $\mathcal{R}_{\mu\nu\rho\sigma}$ and $\mathcal{L}_{\rm matter}$ are the n-dimensional scalar curvature, Ricci tensor, Riemann curvature and the matter Lagrangian, respectively. This action reproduces the standard n-dimensional Einstein gravity, if we set the coupling constant $\alpha_{\rm GB}$ equals to zero.

The action (24) gives the gravitational equation as

$$\alpha_{\rm GR}G_{\mu\nu} + \alpha_{\rm GB}H_{\mu\nu} + g_{\mu\nu}\Lambda = \kappa^2\, T_{\mu\nu}\,, \tag{25}$$

where

$$G_{\mu\nu} = \mathcal{R}_{\mu\nu} - \frac{1}{2}g_{\mu\nu}\mathcal{R}, \tag{26}$$

$$H_{\mu\nu} = 2\Big[\mathcal{R}\mathcal{R}_{\mu\nu} - 2\mathcal{R}_{\mu\alpha}\mathcal{R}^{\alpha}{}_{\nu} - 2\mathcal{R}^{\alpha\beta}\mathcal{R}_{\mu\alpha\nu\beta} + \mathcal{R}_{\mu}{}^{\alpha\beta\gamma}\mathcal{R}_{\nu\alpha\beta\gamma}\Big] - \frac{1}{2}g_{\mu\nu}\mathcal{L}_{\rm GB}, \tag{27}$$

$$T_{\mu\nu} = -2\frac{\delta\mathcal{L}_{\rm matter}}{\delta g^{\mu\nu}} + g_{\mu\nu}\mathcal{L}_{\rm matter}. \tag{28}$$

The higher-order curvature terms are considered as correction terms from string theory. These terms are known to produce two solution branches normally, only one of which has general-relativity limit. The theory is expected to have singularity-avoidance features in the context of gravitational collapses and/or cosmology, but as far as we know there is no studies so far using fully numerical evolutions. (Numerical studies on critical phenomena are recently reported for small $\alpha_{\rm GB}$ [17, 18, 19]).

Studies on wormholes in Gauss-Bonnet gravity have long histories. Several solutions and their classifications are reported in [20, 21], while their energy conditions are considered in [14]. Similar researches are extended to the Lovelock gravity[22], and also to the dilatonic Gauss-Bonnet system [23].

3.2. Dual-null evolution system

We implemented our evolution code [7] for higher-dimensional space-time, and with Gauss-Bonnet gravity terms. The system we consider is spherical symmetry, and expressed using dual-null coordinate. The use of dual-null coordinate simplifies the treatment of horizon dynamics and radiation propagation clearly.

We adopt the line element

$$ds^2 = -2e^{f(x^+,x^-)}dx^+\,dx^- + r^2(x^+,x^-)\gamma_{ij}dz^i dz^j, \tag{29}$$

where the coordinate (x^+, x^-) are along to null propagation directions, and $\gamma_{ij}dx^i dx^j$ is the metric of the $(n-2)$-dimensional unit constant curvature space with $k = \pm 1,\ 0$.

For writing down the Einstein equations, we introduced the variables

$$\Omega = \frac{1}{r}, \tag{30}$$
$$\vartheta_\pm = (n-2)\partial_\pm r \tag{31}$$
$$\nu_\pm = \partial_\pm f \tag{32}$$

which are conformal factor, expansions, and in-affinities, respectively. We also define

$$\eta = \Omega^2\frac{(n-2)(n-3)}{2}\left(ke^{-f} + \frac{2}{(n-2)^2}\vartheta_+\vartheta_-\right). \tag{33}$$

The non-zero Einstein tensor components, then, are

$$G_{++} = -\Omega(\partial_+\vartheta_+ + \vartheta_+\nu_+), \tag{34}$$
$$G_{--} = -\Omega(\partial_-\vartheta_- + \vartheta_-\nu_-), \tag{35}$$
$$G_{+-} = \Omega\partial_-\vartheta_+ + \eta, \tag{36}$$
$$G_{ij} = \gamma_{ij}\left\{e^f\left[\frac{\partial_+\nu_-}{\Omega^2} - \frac{2(n-3)}{(n-2)\Omega}\partial_-\vartheta_+ - \frac{(n-3)(n-4)}{(n-2)^2}\vartheta_+\vartheta_-\right] - k\frac{(n-3)(n-4)}{2}\right\} \tag{37}$$

The EGB equation, (25), becomes

$$\partial_+\vartheta_+ = -\vartheta_+\nu_+ + \frac{1}{\alpha_{\rm GR}\Omega}(\alpha_{\rm GB}H_{++} - \kappa^2 T_{++}), \tag{38}$$
$$\partial_-\vartheta_- = -\vartheta_-\nu_- + \frac{1}{\alpha_{\rm GR}\Omega}(\alpha_{\rm GB}H_{--} - \kappa^2 T_{--}), \tag{39}$$
$$\partial_-\vartheta_+ = \partial_+\vartheta_- = -\frac{\eta}{\Omega} + \frac{1}{\alpha_{\rm GR}\Omega}(\kappa^2 T_{+-} - \alpha_{\rm GB}H_{+-} + e^{-f}\Lambda), \tag{40}$$
$$\begin{aligned}\partial_+\nu_- = \partial_-\nu_+ &= -\frac{2(n-3)}{(n-2)}\eta + \frac{(n-3)(n-4)}{(n-2)^2}\Omega^2\,\vartheta_+\vartheta_- + k\frac{(n-3)(n-4)}{2e^f}\Omega^2 \\ &\quad + \frac{2(n-3)}{(n-2)}\frac{1}{\alpha_{\rm GR}}(\kappa^2 T_{+-} - \alpha_{\rm GB}H_{+-} + e^{-f}\Lambda) \\ &\quad + \frac{\Omega^2}{e^f\alpha_{\rm GR}}\left(\kappa^2 T_{zz} - \alpha_{\rm GB}H_{zz} - r^2\Lambda\right),\end{aligned} \tag{41}$$

where $H_{\mu\nu}$ components are lengthy and we omit them in this article.

We assume ghost scalar field $\phi(x^+, x^-)$,

$$T_{\mu\nu} = -\partial_\mu\phi\partial_\nu\phi - g_{\mu\nu}\left(-\frac{1}{2}(\nabla\phi)^2 + V(\phi)\right), \tag{42}$$

which obeys the Klein-Gordon equation,

$$\Box\phi = \frac{dV}{d\phi}. \tag{43}$$

If we define scalar momentum as

$$p_\pm = r\partial_\pm\phi = \frac{1}{\Omega}\partial_\pm\phi, \tag{44}$$

then non-zero $T_{\mu\nu}$ components are $T_{++} = -\Omega^2 p_+^2$, $T_{--} = -\Omega^2 p_-^2$, $T_{+-} = e^{-f}V$, and $T_{zz} = -e^f p_+ p_- - \Omega^{-2}V$. The eq. (43) becomes

$$\partial_+ p_- = \left(\frac{1}{n-2} - \frac{1}{2}\right)\Omega\vartheta_+ p_- - \frac{1}{2}\Omega\vartheta_- p_+ - \frac{1}{2e^f\Omega}\frac{dV}{d\phi}, \tag{45}$$

$$\partial_- p_+ = -\frac{1}{2}\Omega\vartheta_+ p_- + \left(\frac{1}{n-2} - \frac{1}{2}\right)\Omega\vartheta_- p_+ - \frac{1}{2e^f\Omega}\frac{dV}{d\phi}. \tag{46}$$

These equations complete the system.

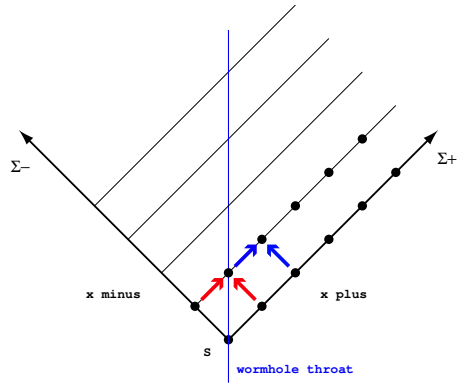

Figure 3. Numerical grid structure. Initial data are given on null hypersurfaces $\Sigma_\pm$ ($x^\mp = 0$, $x^\pm > 0$) and their intersection S. [7].

The basic idea of numerical integration is as follows. We prepare our numerical integration range as drawn in Figure 3. The grid will cover both universes connected by the wormhole throat $x^+ = x^-$. We give initial data on a surface S and the two null hypersurfaces $\Sigma_\pm$ generated from it. Generally the initial data have to be given as

$$(\Omega, f, \vartheta_\pm, \phi) \quad \text{on } S\text{: } x^+ = x^- = 0 \tag{47}$$

$$(\nu_\pm, p_\pm) \quad \text{on } \Sigma_\pm\text{: } x^\mp = 0,\ x^\pm > 0. \tag{48}$$

We then evolve the data $u = (\Omega, \vartheta_\pm, f, \nu_\pm, \phi, p_\pm)$ on a constant-x^- slice to the next.

Due to the dual-null decomposition, the causal region of a grid is clear, and there are in-built accuracy checks: the integrability conditions or consistency conditions $\partial_-\partial_+ u = \partial_+\partial_- u$. In order to update a point N (north), we have two routes from the points E (east) and W (west). The set of equations, (38)-(41) and (45)-(46), gives us x^+-direction (W to N) and x^--direction (E to N) integrations together with the consistency conditions.

As a virtue of the dual-null scheme, we can follow the wormhole throat or black-hole horizons easily. They are both trapping horizons, hypersurfaces where $\vartheta_+ = 0$ or $\vartheta_- = 0$ [24, 25]. Another benefit is the singular point excision technique, since the causal region of each grid point is apparent. When a grid point is inside a black-hole horizon and near to the singularity, we can exclude that point and grid points in its future null cone from further numerical computation.

In order to evaluate the energy, we apply the Misner-Sharp mass in n-dimensional EGB gravity[14],

$$E_n = \frac{(n-2)A_{n-2}}{2\kappa_n^2}\Omega\left[-\frac{1}{\Omega^2}2\frac{\Lambda}{(n-1)(n-2)}+\left(k+\frac{2}{(n-2)^2}e^f\vartheta_+\vartheta_-\right)\right.$$
$$\left.+(n-3)(n-4)\alpha_{\rm GB}\Omega^2\left(k+\frac{2}{(n-2)^2}e^f\vartheta_+\vartheta_-\right)^2\right]. \quad (49)$$

3.3. Evolutions of 4, 5, and 6-dimensional wormhole solutions in GR

We checked our numerical code whether it reproduces the static wormhole solution, obtained in §2. We express our n-dimensional Ellis wormhole solutions in dual-null coordinate and evolved. We find that numerical truncation error can quite easily destroy the stability, but this stability can be controlled with fine resolution. All the results below are obtained after we confirmed the resolution of the code which does not destroy the stability of wormhole throat structure by numerical errors within the evolution (in x^--direction) shown in the figure.

We put perturbations of the static wormhole in the form of Gaussian pulses, input from the right-hand universe. The perturbation is put in the scalar field momentum on its initial data on Σ_+

$$\delta p_+ = c_1\ \exp(-c_2(l-c_3)^2), \quad (50)$$

with all the other initial data as the the static wormhole solution. Here c_1, c_2, c_3 are parameters, and we show the cases with small amplitude and width $c_1 = \pm 0.01$ and $c_2 = 3$, and the initial location $c_3 = 1$. That is, the pulse will hit the wormhole throat at $x^+ = x^- = 1$. Positive (or negative) c_1 corresponds enhancing (or reducing) the supporting ghost field.

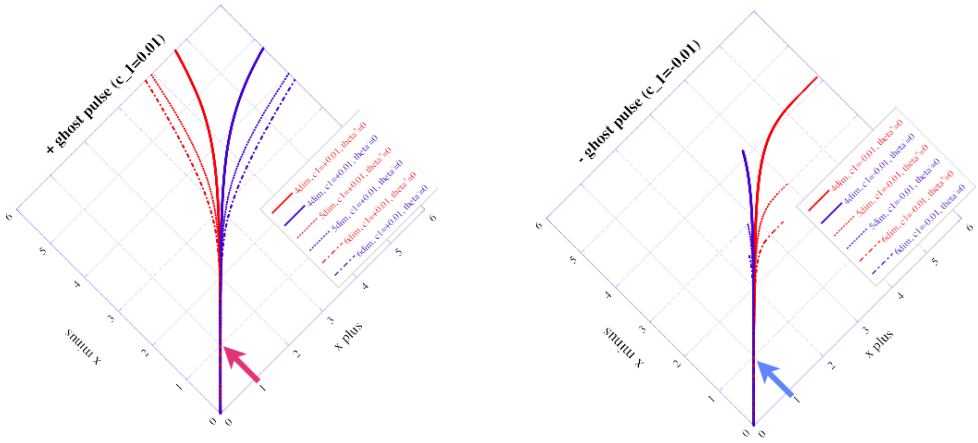

Figure 4. Location of the expansion ϑ_+ (red lines) and ϑ_- (blue lines) for evolutions of a solution in 4, 5, and 6-dimensional General Relativity ($\alpha_{\rm GB} = 0$) as a function of (x_+, x_-). The throat begins expanding if we input negative energy scalar flux (left panel), while the throat turns to be a black hole if we input positive energy scalar flux (right panel).

Figure 4 shows the results of $n = 4, 5$, and 6 dimensional wormhole solution with above perturbation. The plot shows where the vanishing locations of expansions, $\vartheta_\pm = 0$, in (x^+, x^-) plane. We see first the wormhole throat is the location both $\vartheta_\pm = 0$, but after a small pulse hit

it, then the throat (or horizon) split into two ($\vartheta_+ = 0$ and $\vartheta_- = 0$), depending on the signature of the energy of pulse.

If the location of ϑ_+ is outer (in x^+-direction) than that of ϑ_-, then the region $\vartheta_- < x < \vartheta_+$ is judged as a black-hole. Otherwise the region $\vartheta_+ < x < \vartheta_-$ can be judged as an expanding throat. The throat begins expanding if we input negative energy scalar flux (left panel in Figure 4), while the throat turns to be a black hole if we input positive energy scalar flux (right panel).

3.4. Evolutions of 5-dimensional wormhole solution in EGB gravity

We also evolve the same initial data with Gauss-Bonnet terms $\alpha_{\rm GB} \neq 0$ and study their effects to the evolutions.

Figure 5 shows the case of 5-dimensional EGB gravity. The initial data of wormhole on $\Sigma_\pm = 0$ are obtained numerically, solving the set of equations. The evolutions with $\alpha_{\rm GB} \neq 0$ are quite unstable, and we are hard to keep its static configurations long enough. We see if $\alpha_{\rm GB} > 0$ the throat begins expansion (left panel in Figure 5). On the contrary, if $\alpha_{\rm GB} < 0$, then the throat turns to be black-hole (right panel).

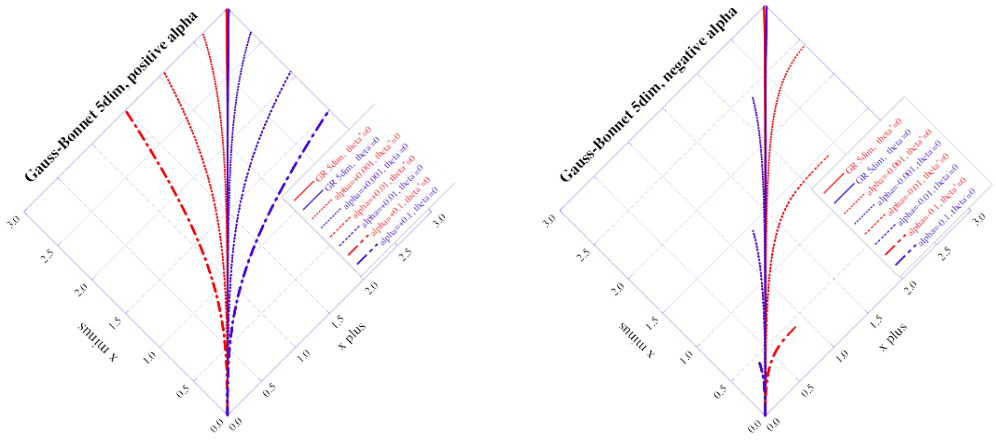

Figure 5. The same with Figure 4, but for 5-dimensional Einstein-Gauss-Bonnet gravity. When $\alpha_{\rm GB} > 0$ (left panel), the throat begins expanding (left panel), while the throat turns to be a black hole for $\alpha_{\rm GB} < 0$ (right panel).

4. Conclusions and Discussions

We studied the simplest wormhole solutions and their stability.

The space-time is assumed to be static and spherically symmetric, has ghost scalar field, and has reflection symmetry at the throat. The four-dimensional version is known to the Ellis (Morris-Thorne) solution, and we derived its extension in the n-dimensional space-time.

Using the linear perturbation technique, we showed that the solutions have at least one negative mode, which concludes that all wormholes are linearly unstable. The time scale of instability becomes shorter as n becomes large.

We, next, confirm the instability with numerical evolutions. Our code uses dual-null coordinate system, which is well-suited for studying horizon structure. At the throat, both the ingoing and outgoing expansions vanish, which means that the throat consists of a degenerate horizon. If we put a small amplitude scalar pulse to the throat, then the wormhole throat

bifurcates, its horizon structure changes into a black-hole or an expanding throat depending the pulse energy is positive or negative, respectively. We also investigated the effect of the higher-order curvature corrections using Gauss-Bonnet terms, and found that such corrections do not work for stabilization of wormholes.

All the behavior of wormholes may be explained simply with energy balance. In [7], for small perturbations, an existence of critical solution is suggested. The similar behaviors are also observed in our investigations, which will be reported elsewhere.

We guess a wormhole with exotic matter is a disguise to avoid public notice, and does prefer to appear as a black-hole or an expanding universe.

Acknowledgments

This work was supported in part by the Grant-in-Aid for Scientific Research Fund of the JSPS (C) No. 25400277. Numerical computations were carried out on SR16000 at YITP in Kyoto University, and on the RIKEN Integrated Cluster of Clusters (RICC).

References

[1] L. Flamm, Physik Z. **17**, 448 (1916).
[2] A. Einstein & N. Rosen, Phys. Rev. **48**, 73 (1935).
[3] M. S. Morris & K. S. Thorne, Am. J. Phys. **56**, 395 (1988).
[4] H. G. Ellis, J. Math. Phys. **14**, 395 (1973).
[5] M. Visser, *Lorentzian Wormholes* (AIP Press, 1995).
[6] F. S. N. Lobo, in *Classical and Quantum Gravity Research* (Nova Sci. Pub., 2008). [arXiv:0710.4474]
[7] H. Shinkai & S.A. Hayward, Phys. Rev. D **66**, 044005 (2002).
[8] A. Doroshkevich, J. Hansen, I. Novikov, & A. Shatskiy, Int. J. Mod. Phys. D **18**, 1665 (2009)
[9] J. A. Gonzalez, F. S. Guzman & O. Sarbach, Class. Quant. Grav. **26**, 015010, 015011 (2009); Phys. Rev. D **80**, 024023 (2009). O. Sarbach & T. Zannias, Phys. Rev. D **81**, 047502 (2010).
[10] S A Hayward, Int. J. Mod. Phys. D **8**, 373 (1999).
[11] B. Zwiebach, Phys. Lett. B **156**, 315 (1985).
[12] A. Chodos & S. Detweiler, Gen. Rel. Grav. **14**, 879 (1982).
[13] G. Clément, Gen. Rel. Grav. **16**, 131 (1984).
[14] H. Maeda & M. Nozawa, Phys. Rev. D **78**, 024005 (2008).
[15] P. Kanti, B. Kleihaus & J. Kunz, Phys. Rev. Lett. **107**, 271101 (2011); Phys. Rev. D **85**, 044007 (2012).
[16] T. Torii & H. Shinkai, Phys. Rev. D **88**, 064027 (2013).
[17] S. Golod & T. Piran, Phys. Rev. D **85**, 104015 (2012).
[18] F. Izaurieta & E. Rodriguez, Class. Quant. Grav. **30** 155009 (2013).
[19] N. Deppe, C. D. Leonard, T. Taves, G. Kunstatter, & R. B. Mann, Phys. Rev. D **86**, 104011 (2012).
[20] B. Bhawal & S. Kar, Phys. Rev. D **46**, 2464 (1992).
[21] G. Dotti, J. Oliva & R. Troncoso, Phys. Rev. D **76**, 064038 (2007).
[22] M H Dehghani & Z Dayyani, Phys. Rev. D**79**, 064010 (2009).
[23] P Kanti, B Kleihaus & J Kunz, Phys. Rev. Lett **107**, 271101 (2011); Phys. Rev. D **85**, 044007 (2012).
[24] S A Hayward, Class. Quant. Grav. **15**, 3147 (1998).
[25] S A Hayward, Phys. Rev. D **49**, 6467 (1994).